In-Situ ATR-FTIR Spectroscopic Study of Electro-oxidation of Methanol and Adsorbed CO at Pt−Ru Alloy

Takahiro Yajima,[†] Hiroyuki Uchida,[†] and Masahiro Watanabe*[,‡]

Graduate School of Engineering, Clean Energy Research Center, University of Yamanashi, Takeda 4, Kofu 400-8511, Japan

Received: October 24, 2003; In Final Form: December 26, 2003

Methanol oxidation reaction (MOR) has been investigated at sputtered Pt−Ru, Ru, and Pt electrodes by using in-situ FTIR spectroscopy with the attenuated total reflection technique (ATR), which can identify species adsorbed on the electrode surface. Linear CO, bridged CO, and COO^- were detected as the intermediates in the MOR. The electro-oxidation of preadsorbed CO was also studied to clarify the mechanism of the MOR at these electrodes. Water molecules coadsorbed with CO were clearly detected at Pt−Ru and Ru electrodes at less positive potential region below the onset potential of ca. 400 mV vs RHE for the electro-oxidation of both methanol and preadsorbed CO. The IR-band intensities of both the adsorbed CO and water commenced to decrease simultaneously at ca. 400 mV on Pt−Ru alloy, demonstrating that the adsorbed CO is oxidized by consuming the adsorbed water. The pure Ru electrode exhibited a high activity for the oxidation of preadsorbed CO, but showed a low activity for the MOR due to the slow dehydrogenation adsorption of the methanol. It is clarified that Pt sites on the alloy surface dehydrogenate methanol and form CO dominantly while Ru sites adsorb water molecules preferentially as oxygen-species needed for the CO oxidation, presumably involved as Ru−OH formed by discharging the adsorbed water. These results support the "bifunctional mechanism" at Pt−Ru alloy for the oxidation of methanol and CO.

1. Introduction

Direct methanol fuel cells (DMFCs) have attracted a great interest as power sources, e.g., for portable devices or relatively small carriers because of their high power densities, simple system (no additional equipment such as fuel reformer) and ease of maintenance. In DMFCs, methanol aqueous solution is directly fed to the anode and electrochemically oxidized. The overall reaction for the methanol oxidation reaction (MOR) is

$$CH_3OH + H_2O \rightarrow CO_2 + 6H^+ + 6e^- \quad (E^\circ = 0.016\ \text{V vs SHE at 25 °C}) \quad (1)$$

At a Pt anode, an overpotential of several hundred millivolts is required to obtain reasonable current density because the adsorbed intermediates such as CO are difficult to be oxidized.[1−3] It has been reported that the MOR rate is significantly enhanced when Pt is alloyed with Ru, Sn, Mo, etc.[4−9] So far, the enhanced activities of these alloy anodes were explained by a bifunctional mechanism[5,6] or a ligand (electronic) effect.[10] It is essential to clarify the mechanism in order to design new electrocatalysts with higher activity.

In-situ infrared spectroscopy combined with the electrochemical method is a powerful tool for studies of the mechanism of such electrochemical reaction. It can, in principle, identify the adsorbed species formed during the MOR. Linear bonded CO,[2,3,11,12] bridged CO,[3,12−14] HCHO,[12] and HCOOH[12] were observed at Pt-base electrodes by using infrared reflection absorption spectroscopy (IRAS). However, we have to notice that there is still much controversy about the reaction mechanism of the MOR even at the Pt electrode. Most of those IRAS studies on the MOR at Pt-base electrodes employed an external reflection setup, in which the infrared beam has to pass through a thick electrolyte solution layer before striking the working electrode surface. The effect of the bulk methanol solution cannot be excluded completely, and a few hundred or thousand interferograms are often required to obtain the data with a high signal-to-noise ratio. To minimize the thickness of the electrolyte solution layer, the working electrode is pressed against the prism. However, the electrochemical response is relatively slow since this arrangement results in a delay of mass transport and a high ohmic resistance. Recently, Osawa and co-workers reported a series of IR spectra obtained on Au or Pt electrode surfaces in aqueous electrolyte solution, utilizing the attenuated total reflection technique (ATR).[15−17] The electrochemical response of the ATR-FTIRS cell is much faster than that in the conventional cell.

Using the ATR-FTIRS technique, we successfully observed the electro-oxidation of the CO ad-layer incorporating with adsorbed water at a pure Pt and a Pt−Fe alloy film electrode.[13,14] Recently, we, for the first time, have reported distinct IR spectra of the adsorbed water together with the reaction intermediates in the MOR at the Pt−Ru alloy electrode using the ATR-FTIRS.[18] In the present paper, we investigated the oxidation reactions of both methanol and adsorbed carbon monoxide in more detail at the Pt−Ru electrode by using the ATR−FTIRS and compared the results with those obtained at pure Pt and pure Ru. The present results give a clue for designing new electrocatalysts for DMFCs.

* Author to whom correspondence should be addressed. Telephone: +81-55-220-8620. Fax: +81-55-254-0371. E-mail: m-watanabe@yamanashi.ac.jp.
[†] Graduate School of Engineering.
[‡] Clean Energy Research Center.

10.1021/jp037215q CCC: $27.50
Published on Web 02/03/2004

2. Experimental Section

The configuration of the spectro-electrochemical cell used in the present work was similar to that described in our previous works.[3,13,14] Thin-film PtRu alloy, pure Pt, or Ru working electrodes (about 10 nm in thickness) were prepared on the flat plane of a silicon hemicylindrical prism by Ar-sputtering Pt and/or Ru targets at room temperature. The resulting alloy composition determined by a fluorescent X-ray analysis (EDX-800, Shimadzu) was $Pt_{50}Ru_{50}$. X-ray diffraction patterns of the Pt−Ru alloy indicated the formation of a solid solution with a face-centered cubic (fcc) crystal structure. The metal-coated prism was attached to the spectro-electrochemical cell by sandwiching an O-ring. The geometrical surface area of the working electrode was about 1.77 cm^2.

Solution of 0.1 M $HClO_4$ with and without 1 M CH_3OH was prepared from reagent grade chemicals (Kanto Chemical Co. Japan) and Milli-Q water. The supporting electrolyte solution of 0.1 M $HClO_4$ was purified with conventional methods.[19,20] All electrode potentials are reported with respect to the reversible hydrogen electrode (RHE). Before the collection of spectro-electrochemical data, a cyclic voltammogram for clean working electrode in deaerated 0.1 M $HClO_4$ was obtained. Next, helium gas containing 1% CO was purged into 0.1 M $HClO_4$ solution at 100 mV for 30 min in order to obtain a preadsorbed CO layer on the electrode. CO in the bulk solution was removed by purging with N_2 while keeping the potential constant for 1 h. Then, a cyclic voltammogram and infrared spectra for the oxidation of adsorbed CO were simultaneously obtained. Following this measurement, methanol was added into the solution, keeping the potential at 100 mV for 1 h until a potential sweep and simultaneous spectra acquisitions were started.

Fourier transform infrared (FTIR) spectra were taken with a Bio-rad FTS-6000 spectrometer equipped with a liquid nitrogen cooled linearized narrow-band MCT detector. Unpolarized infrared radiation from a Globar source was focused at the electrode/electrolyte interface by passing it through the silicon prism. The incident angle was 70° from the surface normal. Each spectrum was acquired by integrating only 14 interferograms with a resolution of 8 cm^{-1} during a potential sweep at a rate of 20 mV s^{-1}. Since the acquisition time was 2.5 s per spectrum, each spectrum is the average of every 50 mV interval. The spectrum at 975 mV was chosen as the reference.

3. Results and Discussion

3.1. Adsorbed CO Oxidation. First, an electro-oxidation reaction of preadsorbed CO (CO_{ad}) at Pt, Ru, or Pt−Ru was investigated, because this is a well-known key reaction step in the MOR. Figure 1 shows cyclic voltammograms with (solid curve) and without (dashed curve) CO_{ad} at Pt−Ru, Pt, and Ru in 0.1 M $HClO_4$. In the positive-going scan at pure Pt electrode, a major CO_{ad} oxidation peak is observed at about 0.7 V after a small preoxidation peak at 0.5 V. On the other hand, the anodic current for the CO_{ad} oxidation commences to increase at about 400 mV at both Pt−Ru and pure Ru electrodes. This indicates that Pt−Ru alloy and pure Ru have higher activity for the CO_{ad} oxidation than pure Pt, being consistent with many other studies so far.[19,21−24]

Figure 2 shows in-situ ATR-FTIR spectra simultaneously acquired with the CV for the CO_{ad} oxidation at the Pt−Ru (A), the Pt (B), and the Ru (C) electrodes, respectively. Observed IR bands and their assignments are summarized in Table 1. At a low potential region less positive than the onset potential (E_{onset}) on the Pt−Ru (see Figure 1), strong bipolar-shaped bands and some positive bands are observed at 2080 to 1800 cm^{-1},

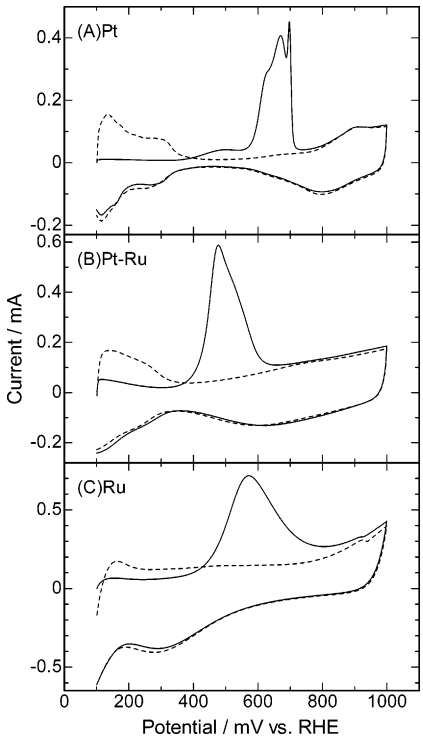

Figure 1. CVs for the oxidation of preadsorbed CO at $Pt_{50}Ru_{50}$ (A), Pt (B), and Ru (C) electrodes in 0.1 M $HClO_4$. Dashed curves are CVs for these electrodes without CO_{ad}. Sweep rate was 20 mV s^{-1}.

TABLE 1: Observed IR Bands and Their Assignments in Figure 2

	wavenumber/cm^{-1}		
assignment	Pt−Ru	Pt	Ru
CO_L	2060−2025	2080−2060	2025−1995
CO_B	∼1800	1880−1840	∼1800
H_2O_{ad}, ν(OH)	3620−3607		3634−3615
H_2O_{ad}, δ(HOH)	∼1616		∼1615

which can be assigned to adsorbed CO species. The strong bipolar bands at 2025−2060 cm^{-1} are assigned to the stretching mode of linearly bonded CO (CO_L) at Pt site.[2,3,11−14] The bipolar shape of the CO_L bands is consistent with that in our recent papers studied on the oxidation of adsorbed CO and methanol at Pt electrode.[3,13] The asymmetric shape of the band can be attributed to some physical effect originated from a property and/or a structure of the electrode.[3,26−29] A small shoulder band around 1950 cm^{-1} can be assigned to CO_L adsorbed at Ru sites.[22,25,30] A small band around 1800 cm^{-1} can be assigned to the stretching mode of bridge-type CO (CO_B).[3,12−14] At the pure Pt electrode, bands at 2080−2060 cm^{-1} (bipolar) and 1880−1840 cm^{-1} are assigned to CO_L and CO_B, respectively.[2,3,11−14] At the pure Ru electrode, CO_L and CO_B bands are seen at 2025−1995 cm^{-1} and about 1800 cm^{-1}.[22,25]

At the Pt−Ru surface, distinct positive-going bands at 3620−3607 cm^{-1} and about 1616 cm^{-1} are clearly observed at less positive potential region. As we reported in the previous work for the MOR at Pt−Ru,[18] these bands are assigned to the stretching mode and the bending mode of adsorbed water. The wavenumbers of them are quite different from those of bulk water, but are rather similar to those of water monomer, i.e., the hydrogen bonding between the water molecules is negligibly weak.[31−33] According to the surface selection rule, the water is adsorbed on the surface with its C_2 axis perpendicular to the surface.[32,33] Because similar bands of the adsorbed water can be identified at the pure Ru electrode [Figure 2C, ν(OH);

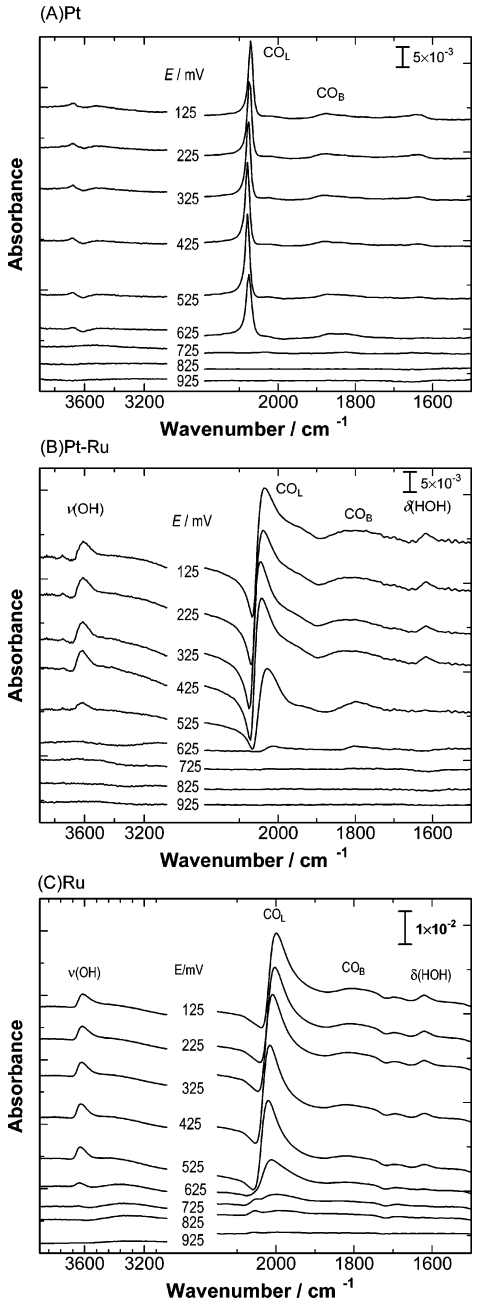

Figure 2. In-situ ATR-FTIR spectra for the oxidation of preadsorbed CO at Pt (A), $Pt_{50}Ru_{50}$ (B), and Ru (C) electrodes in 0.1 M $HClO_4$. The spectrum acquired at 975 mV at each electrode was taken as a reference.

3634−3615 cm^{-1}, δ(HOH); 1615 cm^{-1}] but hardly observed at the pure Pt electrode (Figure 2A), water molecules probably adsorb at Ru sites on the Pt−Ru alloy. Such distinct bands for the adsorbed water cannot be observed at CO-free surface of Pt−Ru (Figure 3B) or Ru (Figure 3C) similar to pure Pt (Figure 3A), where water molecules on the surfaces are dominantly hydrogen-bonded. These results strongly indicate that adsorbed CO molecules weaken the hydrogen bonding among water molecules at Ru−Pt alloy and Ru surfaces, resulting in the formation of isolated water molecules on Ru sites surrounded by adsorbed CO molecules. This distinctive behavior from pure Pt is brought by a higher affinity of Ru to the water adsorption than pure Pt in the presence of adsorbed CO on the surface. An interaction between CO_{ad} and adsorbed water at Pt−Ru or Ru can be supported further as follows. As seen in Figure 2, the wavenumber of C−O stretching at the Pt−Ru and the Ru is

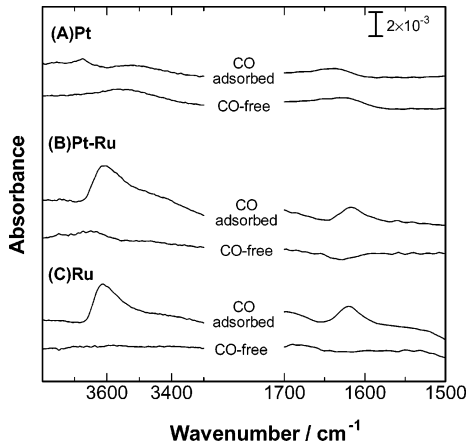

Figure 3. Comparison of IR spectra (typical region for ν(OH) and δ(HOH) of water) for CO-free and CO adsorbed surfaces at Pt (A), $Pt_{50}Ru_{50}$ (B), and Ru (C) electrodes at 125 mV in 0.1 M $HClO_4$. The spectrum acquired at 975 mV at each experiment was taken as a reference.

lower than that at the pure Pt. Note that this result does not directly mean a higher bond strength between CO and metal (Pt−Ru, Ru) than that of CO and pure Pt. Ito et al. reported that the wavenumber of CO_L adsorbed on Ru(0001) in the UHV was decreased by coadsorption with water (D_2O).[34,35] Such a red-shift was ascribed to an electron transfer from water to Ru and/or the reduced lateral interaction between CO molecules.[34,35] Further study is needed to explain such a red-shift of the CO band at Ru−Pt alloy or Ru electrode surfaces, but this is the experimental fact. It is also a clear fact that water molecules can be adsorbed on the surface of Pt−Ru and Ru electrodes together with CO_{ad} at the potential region less positive than the onset potential of CO oxidation.

As shown in Figure 3A, broad bands at about 3500 and 1610 cm^{-1} are observed at pure Pt in the CO-free blank solution at 125 mV, which can be assigned to ν(OH) and δ(HOH) of water, respectively. Their intensities decreased and the bands showed red-shift with the increase of potential (not shown in this figure). This suggests the potential-induced change of the orientation of water near the surface. At CO-adsorbed Pt, a weak and abnormal shape IR band, assigned to ν(OH) of water, appears from 3500 to 3700 cm^{-1} (Figure 2A), which is quite different from those observed at the Pt−Ru or Ru electrode. The depression of the ν(OH) band around 3600 cm^{-1} in Figure 2A may be ascribed to a partial exclusion of the water from the surface by the strong adsorption of CO molecules at the pure Pt. Thus, at low potential region, the Pt surface is almost fully covered by CO_{ad}, whereas the Pt−Ru and the Ru adsorb water molecules together with CO_{ad}.

Figure 4 shows potential dependence of IR band intensities of CO_L and ν(OH) of the adsorbed water and the oxidation current of CO_{ad} in the positive-going scan at Pt−Ru, Pt, and Ru electrodes. It is noted that the band intensities of CO_L and adsorbed water commence to decrease together at about 400 mV on Pt−Ru and Ru, responding to the rapid increase of the oxidation current. Thus, it becomes clear by the present ATR-FTIRS measurement on Pt−Ru alloy and Ru that the adsorbed CO is oxidized by consuming the adsorbed water. However, it must be noted that the electro-oxidation of adsorbed CO cannot occur at less positive potential than 400 mV even though such water molecules are already adsorbed together with CO at Pt−Ru and Ru surface. This indicates that adsorbed water molecules cannot directly oxidize CO molecules. Accordingly, we consider the following reaction scheme.

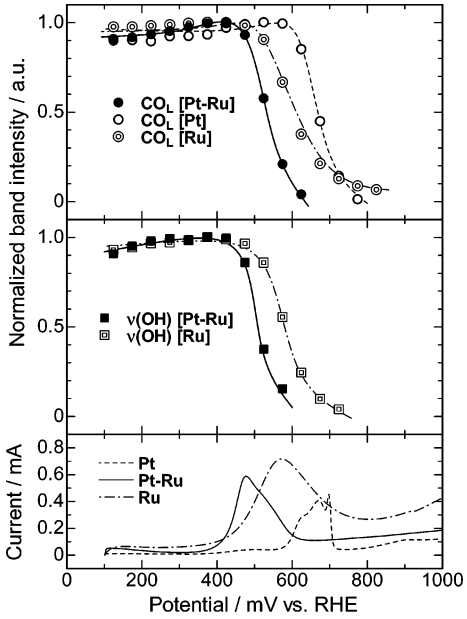

Figure 4. Potential dependence of normalized IR intensity of CO_L and ν(OH) of adsorbed water obtained from Figure 2. With respect to the bipolar band of CO at the Pt−Ru and the Ru, the peak-to-peak height was taken to calculate the intensity.

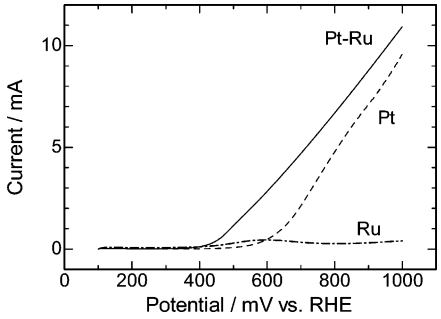

Figure 5. Linear sweep voltammograms for the MOR at $Pt_{50}Ru_{50}$, Pt, and Ru electrodes in 1 M CH_3OH + 0.1 M $HClO_4$ solution. Scan rate was 20 mV s^{-1}.

First, active species such as Ru−OH may be formed since water molecules adsorbed on Ru sites can discharge at less positive potential (about 400 mV) as previously supposed in the literatures.

$$Ru-OH_2 \rightarrow Ru-OH + H^+ + e^- \quad (2)$$

Once the Ru−OH is formed, the adsorbed CO is easily oxidized to CO_2, as indicated by the simultaneous reduction of IR-bands of both the adsorbed water and CO.

$$Pt-CO + Ru-OH \rightarrow Pt + Ru + CO_2 + H^+ + e^- \quad (3)$$

This reaction mechanism is the so-called "bifunctional mechanism" for the oxidation of CO_{ad}, proposed by Watanabe and Motoo.[5,6] The present in-situ spectroscopic results elucidate the roll of the Ru toward the oxidation of adsorbed CO.

3.2. Methanol Oxidation Reaction. Figure 5 shows linear sweep voltammograms (LSVs) for the MOR at Pt−Ru (solid curve), Pt (dashed curve), and Ru (dash−dotted curve) electrodes in 1 M CH_3OH + 0.1 M $HClO_4$ solution. The methanol oxidation current commences to increase at E_{onset} = ca. 400 mV at the Pt−Ru, while E_{onset} at the Pt was about 600 mV. The E_{onset} for the MOR at these two electrodes is almost the same as that for the oxidation of CO_{ad} shown in Figure 1. Thus,

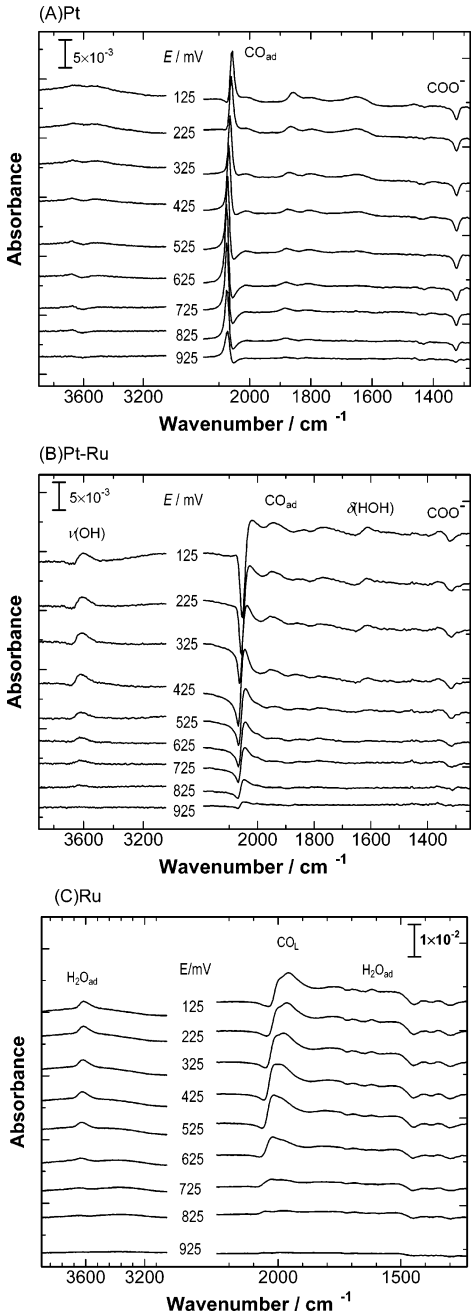

Figure 6. In-situ ATR-FTIR spectra for the MOR at Pt (A), $Pt_{50}Ru_{50}$ (B), and Ru (C) electrodes in 1 M CH_3OH + 0.1 M $HClO_4$ solution. The spectrum acquired at 975 mV at each electrode was taken as a reference.

it is indicated that the rapid increase in the MOR current strongly corresponds to the oxidation of the poisoning intermediate CO. At the Ru electrode, however, no appreciable current of methanol oxidation is observed even at high potential region, although the Ru indeed exhibited high activity for the CO_{ad} oxidation. Coupled with the voltammograms, in-situ FTIR measurement provides more detailed information about the MOR.

Figure 6 shows in-situ ATR-FTIR spectra simultaneously acquired with the LSV for the MOR at Pt−Ru, Pt, and Ru electrodes. Table 2 summarizes the observed IR bands and their assignments. Strong bands at 2080−1800 cm^{-1}, which are assigned to adsorbed CO species, are observed already at 125 mV on the Pt−Ru and Pt, indicating that methanol is dehydrogenated to CO while keeping the potential at 100 mV.

TABLE 2: Observed IR Bands and Their Assignments in Figure 6

	wavenumber/cm^{-1}		
assignment	Pt−Ru	Pt	Ru
CO_L	2060−1950[a]	2075−2056	2010−1950
CO_B	∼1800	1880−1840	∼1820
H_2O_{ad}, ν(OH)	3620−3600		3630−3615
H_2O_{ad}, δ(HOH)	∼1615		∼1618
$\nu_s(COO^-)$	∼1325	∼1319	

[a] CO_L−Pt (2060−2015 cm^{-1}) and CO_L−Ru (∼1950 cm^{-1}).

At the Pt−Ru electrode, the strong bipolar bands at 2030−2050 cm^{-1} are assigned to CO_L at the Pt site. A distortion of the shape of CO_L is ascribed to not only the physical origin described above but also the subtraction of the reference spectrum taken at 975 mV, since we cannot completely exclude the existence of a small amount of CO in the reference spectrum. Bands of 1940 to 2000 cm^{-1} can be assigned to CO_L adsorbed at Ru sites. At the Pt, CO_L and CO_B appear at 2075−2056 cm^{-1} and 1880−1840 cm^{-1}, respectively. At the Ru, CO_L and CO_B appear at 2010−1950 cm^{-1} and about 1820 cm^{-1}, respectively, and the intensity of CO_L is smaller than that at CO preadsorbed Ru. The CO_L band at the Ru seems to consist of two peaks. Such a splitting of the CO_L band was reported by Lin et al. at Ru(0001) with an intermediate CO coverage, i.e., the packed island of CO_L (higher frequency) and loose CO_L (lower frequency).[25] Therefore, the CO coverage was low even when the potential was kept at 100 mV for 1 h in the presence of methanol. Bands for ν(OH) and δ(HOH) of the adsorbed water at the Ru site are also observed at the Pt−Ru [ν(OH): 3620−3600 cm^{-1}, δ(HOH): ∼1615 cm^{-1}], and the Ru [ν(OH): 3630−3615 cm^{-1}, δ(HOH): ∼1618 cm^{-1}] for the MOR. Hence, very low MOR activity at the pure Ru shown in Figure 5 can be ascribed to the low dehydrogenation rate of methanol to form CO_{ad}.

Negative bands at about 1320 cm^{-1}, which can be assigned to the symmetric stretching of OCO of COO^- group, are observed at the Pt−Ru (1325 cm^{-1}) and the Pt (1319 cm^{-1}).[11,22] Since the spectrum at 975 mV was taken as reference, the height reduction in the negative bands with increasing potential implies the formation of COO^- at a higher potential region. Recently, Osawa et al. observed the band at almost the same wavenumber in 0.1 M CH_3OH + 0.1 M $HClO_4$ at the electroplated Pt. They claimed it being assigned to an adsorbed formate ($HCOO^-$), although the formation mechanism was not clearly shown.[16,17] Although further experiments are necessary to clarify the intermediates at high potential region, we might be able to consider the following stepwise reaction schemes for the formation of COO^- on Pt−Ru alloy electrode.

$$Pt{-}CO + Ru{-}OH \rightarrow Pt{-}COO^- + Ru + H^+ \quad (3\text{-}1)$$

$$Pt{-}COO^- \rightarrow Pt + CO_2 + e^- \quad (3\text{-}2)$$

The formation of COO^- on pure Pt electrode at higher potential can also be explained by replacing Ru−OH with Pt−OH and Ru with Pt, respectively, in the eq 3-1.

Figure 7 shows the potential-dependence of the normalized IR-band intensity of each adsorbed species and the voltammograms for the methanol oxidation at the Pt−Ru alloy and at the Pt electrode. Similar to the case of the CO_{ad} oxidation, it is striking that the band intensities of both CO_L and adsorbed water commence to decrease together steeply on the Pt−Ru alloy at about 400 mV, i.e., the E_{onset} for MOR. This is a clear demonstration of that the adsorbed CO, which is the dominant

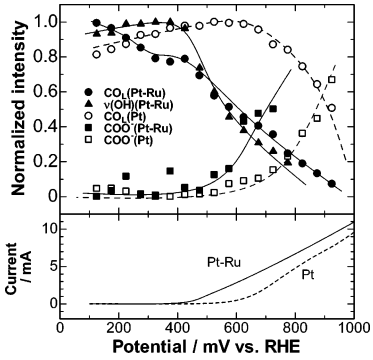

Figure 7. Potential dependence of normalized IR intensity of CO_L, $\nu(COO^-)$ and ν(OH) of adsorbed water obtained from Figure 6. The peak-to-peak height was taken to calculate the intensity of the bipolar band.

poison in the MOR, is oxidized by consuming the activated adsorbed water described above. It is seen in Figure 7 that the band intensity of CO_L decreases gradually at the Pt−Ru as the potential is increased up to 400 mV despite negligible anodic current. We consider such a change to be ascribed to some artifacts yielded by background subtraction. In the MOR, for example, the CO_L still remained at the surface at the reference potential of 975 mV though the amount is small. Our calculation of the intensity of the CO_L band includes a further error to some extent by the following reason. The peak wavenumber of the CO_L shifts from 2020 to 2040 cm^{-1} with increasing potential from 100 to 400 mV and is almost constant at E > 400 mV. By subtracting the reference spectrum, the bipolar band shape appreciably changes between 100 and 400 mV, which affects the calculation of the peak-to-peak intensity. We would like to emphasize again that the most important point is that the band intensities of both CO_L and adsorbed water commence to decrease together steeply at about 400 mV at the Pt−Ru electrode for both the MOR and the oxidation of CO_{ad}.

On the other hand, the intensity of the COO^- species commences to increase at the potential more positive than the E_{onset} for the MOR at both electrodes (Pt−Ru: about 400 mV, Pt: about 600 mV). It is also noticed that a considerable amount of CO_L remains at very positive potential region, e.g., >0.6 V at Pt−Ru alloy and >0.8 V at pure Pt, whereas preadsorbed CO molecules completely disappeared by the oxidation at such potentials on both electrodes as seen in Figure 4. These results indicate that adsorbed CO is continuously produced by the dehydrogenation of methanol even at such a high potential region and COO^- species may be the oxidation intermediate of methanol or the produced CO at high potential region.

Finally, on the basis of the present ATR-FTIRS measurement, we propose a mechanism of the MOR at Pt−Ru alloy electrode, as shown in Figure 8. While keeping the potential at 100 mV, methanol is dehydrogenated to CO dominantly at the Pt site. The dehydrogenation may proceed stepwise, but any other species (such as HCHO) could not be detected by in-situ ATR-FTIRS, probably due to fast dehydrogenation kinetics to form CO.

$$CH_3OH + Pt \rightarrow CO{-}Pt + 4H^+ + 4e^- \quad (4)$$

Small amounts of other CO_{ad} such as CO_L−Ru or CO_B species are also produced. In the same potential region, water molecules adsorb at Ru sites.

$$H_2O + Ru \rightarrow Ru{-}OH_2 \quad (5)$$

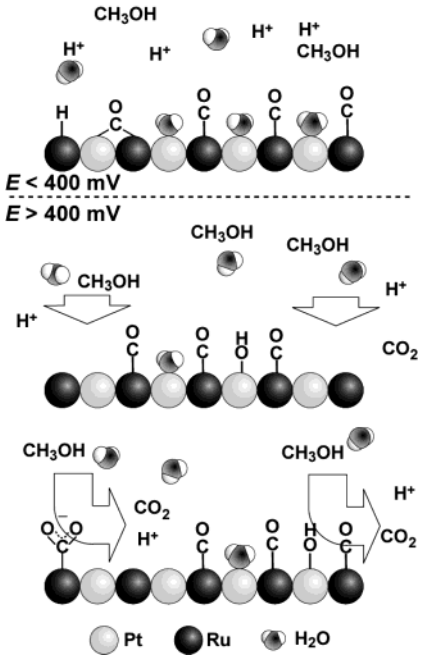

Figure 8. Schematic illustration of the MOR at Pt−Ru electrode.

At about 400 mV, adsorbed water molecules discharge to form Ru−OH.

$$\mathrm{Ru{-}OH_2} \rightarrow \mathrm{Ru{-}OH} + \mathrm{H^+} + \mathrm{e^-} \qquad (2)$$

Ru−OH can rapidly oxidize the poisoning CO_{ad} to CO_2.

$$\mathrm{Pt{-}CO} + \mathrm{Ru{-}OH} \rightarrow \mathrm{Pt} + \mathrm{Ru} + \mathrm{CO_2} + \mathrm{H^+} + \mathrm{e^-} \qquad (3)$$

Equation 3 may consist of the elemental steps of eqs 3-1 and 3-2. This is the "bifunctional mechanism" for the MOR, proposed by Watanabe and Motoo.[5,6] The resulting free Pt sites are available for the continuous oxidation of methanol via CO_{ad} and COO^- species.

4. Conclusions

The present in-situ ATR-FTIR spectroscopy sensitively identifies the adsorbed species such as CO_L, CO_B, COO^-, and particularly adsorbed water during the MOR at the sputtered Pt−Ru film electrode in 1 M CH_3OH + 0.1 M $HClO_4$ solution. Such water molecules are adsorbed at the Ru sites, because they were detected at the pure Ru electrode but at the Pt electrode. CO molecules dominantly adsorbed at Pt sites as dissociative adsorption products from methanol. The IR-band intensities of both water and CO_{ad} commenced to decrease simultaneously at about 400 mV vs RHE (the E_{onset} of the MOR at the Pt−Ru electrode), while additional overpotential of ca. 200 mV was necessary to oxidize the CO_{ad} at Pt electrode. Thus, the oxidation of CO_{ad} is a key step in the MOR at Pt and Pt−Ru alloy. However, the active species to oxidize CO is not the adsorbed water but presumably Ru−OH. We believe that this result will accelerate the development of new DMFC anode catalysts.

Acknowledgment. This work was supported by CREST of Japan Science and Technology (JST) Corporation, and also was supported by the fund for "Leading Project" of Ministry of Education, Science, Culture, Sports and Technology of Japan.

References and Notes

(1) Kunimatsu, K. *J. Electroanal. Chem.* **1982**, *140*, 205.
(2) Persons, R.; VanderNoot, T. *J. Electroanal. Chem.* **1988**, *257*, 9.
(3) Zhu, Y.; Uchida, H.; Yajima, T.; Watanabe, M. *Langmuir* **2001**, *17*, 146.
(4) Arico, A. S.; Srinivasan, S.; Antonucci, V. *Fuel Cells* **2001**, *1*, 133.
(5) Watanabe, M.; Motoo, S. *J. Electroanal. Chem.* **1975**, *60*, 267.
(6) Watanabe, M.; Motoo, S. *Denki Kagaku* **1973**, *41*, 190.
(7) Watanabe, M.; Uchida, M.; Motoo, S. *J. Electroanal. Chem.* **1986**, *199*, 311.
(8) Gasteiger, H. A.; Markovic, N.; Ross, P. N., Jr.; Cairns, E. J. *J. Electrochem. Soc.* **1994**, *141*, 1795.
(9) Ren, X.; Wilson, M. S.; Gottesfeld, S. *J. Electrochem. Soc.* **1996**, *143*, L12.
(10) Frelink, T.; Visscher, W.; van Veen, J. A. R. *Surf. Sci.* **1995**, *335*, 353.
(11) Beden, B.; Lamy, C.; De Tacconi, N. R.; Arvia, A. J. *Electrochim. Acta* **1990**, *35*, 691.
(12) Kabbabi, A.; Faure, R.; Durand, R.; Beden, B.; Hahn, F.; Leger, J.-M.; Lamy, C. *J. Electroanal. Chem.* **1998**, *444*, 41.
(13) Zhu, Y.; Uchida, H.; Watanabe, M. *Langmuir* **1999**, *15*, 8757.
(14) Watanabe, M.; Zhu, Y.; Uchida, H. *J. Phys. Chem. B* **2000**, *104*, 1762.
(15) Osawa, M. *Bull. Chem. Soc. Jpn.* **1997**, *70*, 2861.
(16) Miki, A.; Ye, S.; Osawa, M. *Chem. Commun.* **2002**, 1500.
(17) Chen, Y. X.; Miki, A.; Ye, S.; Sakai, H.; Osawa, M. *J. Am. Chem. Soc.* **2003**, *125*, 3680.
(18) Yajima, T.; Wakabayashi, N.; Uchida, H.; Watanabe, M. *Chem. Commun.* **2003**, 828.
(19) Watanabe, M.; Motoo, S. *J. Electroanal. Chem.* **1975**, *60*, 275.
(20) Uchida, H.; Ikeda, N.; Watanabe, M. *J. Electroanal. Chem.* **1997**, *424*, 5.
(21) Krausa, M.; Vielstich, W. *J. Electroanal. Chem.* **1994**, *379*, 307.
(22) Lin, W. F.; Iwasita, T.; Vielstich, W. *J. Phys. Chem. B* **1999**, *103*, 3250.
(23) Gutiérrez, C.; Caram, J. A.; Beden, B. *J. Electroanal. Chem.* **1991**, *305*, 289.
(24) Friedrich, K. A.; Geyzers, K.-P.; Linke, U.; Stimming, U.; Stumper, J. *J. Electroanal. Chem.* **1996**, *402*, 123.
(25) Lin, W. F.; Christensen, P. A.; Hamnett, A.; Zei, M. S.; Ertl, G. *J. Phys. Chem. B* **2000**, *104*, 6642.
(26) Fano, U. *Phys. Rev. B* **1961**, *124*, 1866.
(27) Holfeld, C. P.; Loser, F.; Sudzius, M.; Leo, K.; Whittaker, D. M.; Kohler, K. *Phys. Rev. Lett.* **1998**, *81*, 874.
(28) Bjerke, A. E.; Griffiths, P. R.; Theiss, W. *Anal. Chem.* **1999**, *71*, 1967.
(29) Lu, G.-Q.; Sun, S.-G.; Chen, S.-P.; Cai, L.-R. *J. Electroanal. Chem.* **1997**, *421*, 19.
(30) Brankovic, S. R.; Marinkovic, N. S.; Wang, J. X.; Adzic, R. R. *J. Electroanal. Chem.* **2002**, *532*, 57.
(31) Kitamura, F.; Nanbu, N.; Ohsaka, T.; Tokuda, K. *J. Electroanal. Chem.* **1998**, *452*, 241.
(32) Ataka, K.; Yotsuyanagi, T.; Osawa, M. *J. Phys. Chem.* **1996**, *100*, 10664.
(33) Ataka, K.; Osawa, M. *Langmuir* **1998**, *14*, 951.
(34) Nakamura, M.; Ito, M. *Chem. Phys. Lett.* **2001**, *335*, 170.
(35) Nakamura, M.; Ito, M. *Surf. Sci.* **2001**, *490*, 301.